BMB Reports - Manuscript Submission

Manuscript Draft

Manuscript Number: BMB-21-118

Title: Translocalization of enhanced PKM2 protein into the nucleus induced by cancer upregulated gene (CUG) 2 confers cancer stem cell-like phenotypes

Article Type: Article

Keywords: CUG2; PKM2; Cancer Stem Cell; Non-Metabolic Function; Co-activator

Corresponding Author: Young-Hwa Chung

Authors: Natpaphan Yawut[1,#], Sirichat Kaowinn[2,#], Il-Rae Cho[3], Phatcharaphon Budluang[4], Seonghye Kim[5], Suhkmann Kim[6], So Eun Youn[7], Sang Seok Koh[8], Young-Hwa Chung[9,*]

Institution: [1]Cogno-Mechatronics Engineering, Pusan National University,
[2]General Science and Liberal Arts, King Mongkut's Institute of Technology,
[3]Chemistry, Pusan National University,
[4]Biomedical Sciences, Dong-A University,

Translocalization of enhanced PKM2 protein into the nucleus induced by cancer upregulated gene 2 confers cancer stem cell-like phenotypes

Natpaphan Yawut[1a], Sirichat Kaowinn[2a], Il-Rae Cho[1], Phatcharaphon Budluang[1], Seonghye Kim[3], Suhkmann Kim[3], So Eun Youn[4], Sang Seok Koh[4], and Young-Hwa Chung[1*]

[1]BK21 plus, Department of Cogno-Mechatronics Engineering, Optomechatronics Research Center, [3]Department of Chemistry, Pusan National University, Busan 46241, Republic of Korea

[2]Department of General Science and Liberal Arts, King Mongkut's Institute of Technology, Ladkrabang Prince of Chumphon Campus, Chumphon 86160, Thailand

[4]Department of Biomedical Sciences, Dong-A University, Busan 49315, Republic of Korea

Keywords: CUG2, PKM2, cancer stem cell, non-metabolic function, co-activator

a; These authors contributed equally to this work

* Corresponding author; Young-Hwa Chung, PhD, Department of Cogno-Mechatronics Engineering, Optomechatronics Research Center, Pusan National University, Busan 46241, Republic of Korea, *Email* ; younghc@pusan.ac.kr

ABSTRACT

Increased mRNAs of *cancer upregulated gene (CUG)2* were detected in many different tumor tissues using the Affymetrix microarray and the oncogenic capability of the *CUG2* gene was further reported. The mechanism by which CUG2 overexpression promotes cancer stem cell (CSC)-like phenotypes, on the other hands, is still unknown. With recent studies showing that pyruvate kinase muscle 2 (PKM2) is overexpressed in clinical tissues from gastric, lung, and cervical cancer patients, we hypothesized that PKM2 plays an important role in CSC-like phenotypes caused by CUG2 overexpression. Herein, compared with the control cells, enhanced PKM2 protein levels and translocation of PKM2 into the nucleus were detected for CUG2-overexpressing lung carcinoma A549 and immortalized bronchial BEAS-2B cells. In the CUG2-overexpressing cells, the expression of c-Myc, CyclinD1, and PKM2 was increased. Furthermore, EGFR and ERK inhibitors as well as the suppression of Yap1 and NEK2 expression reduced PKM2 protein levels. Interestingly, the knockdown of β-catenin expression failed to reduce the PKM2 protein levels. Furthermore, the reduction of PKM2 expression with its siRNA hindered CSC-like phenotypes such as faster wound healing, aggressive transwell migration, increased size and number of sphere formation. The introduction of mutant S37A PKM2-green fluorescence protein (GFP) into cells, that were unable to move to the nucleus, in particular, did not confer CSC-like phenotypes, whereas the forced expression of wild-type PKM2 promoted those phenotypes. Overall, CUG2-induced increased expression of nuclear PKM2 contributes to CSC-like phenotypes via upregulation of c-Myc and CyclinD1 as a co-activator.

INTRODUCTION

Increased *CUG2* transcripts have been detected in many different cancer tissues, using the Affymetrix microarray system, including the lung, ovary, and colon (1). CUG2's oncogenic activity of is demonstrated by enhanced proliferation and tumor formation in nude mice (1). Moreover, the capability of the *CUG2* gene possesses CSC-like phenotypes in terms of rapid cell migration, an aggressive cell invasion, an enhanced sphere forming ability, and an increased doxorubicin-resistance through TGF-β signaling (2), (3). These phenotypes have been linked to both EGFR/Stat1/HDAC4 signaling pathway and the β-catenin/yes-associated protein (Yap1)/NIMA-related kinase 2 (NEK2) signaling pathway (4), (5). According to recent studies, the increased EGFR and β-catenin protein levels and signaling during CUG2 overexpression can be attributed to the decreased Spry2 protein via c-Cbl (6).

In many cases, cancer cells display increased glucose consumption and lactate generation even under aerobic conditions, which are features of Warburg effect, called as aerobic glycolysis (7), (8). In this case, pyruvate kinase muscle 2 (PKM2), a key enzyme of glycolysis pathway, is to be held responsible (7), (8), (9). According to further investigation, PKM2 protein which consists of four structural units (tetramer) has high catalytic activity, resulting in high ATP production and more energetic catabolic metabolism (7), (10). Of interest, dimeric PKM2 protein (two structural units) displays a low catalytic activity, which provides glycolytic intermediates for anabolism (7), (10). PKM2 protein exists in the cytoplasm and is translocated to the nucleus, which suggests that PKM2 has other functions (8), (9), in addition to glycolysis, such as acting as a protein kinase (11). For example, PKM2 protein does not use phosphoenolpyruvate as a metabolic substrate. Rather, PKM2 protein can take away of a phosphate group from the phosphoenolpyruvate and then attach the phosphate group to Stat3

(12), histone H3 (13), and ERK1/2 (14), allowing tumor cells to proliferate. As a co-activator, once translocated to the nucleus, PKM2 protein can bind to HIF-1α protein. Eventually, the complex between PKM2 and HIF-1α contributes to accelerating mRNA synthesis of HIF-1α-targeting genes (15), (16). Furthermore, the protein complex between PKM2 and c-Src can be recruited into a CyclinD1 promoter containing β-catenin, leading to the up-regulation of CyclinD1 transcripts (17), (18).

This investigation was initiated to illustrate a PKM2's role in CUG2-induced tumor development. Both EGFR and ERK1/2 kinases activities contributed to the increased PKM2 protein levels, leading to upregulation of c-Myc and CyclinD1 expression. Furthermore, Yap1 and NEK2 increased the PKM2 protein expression, while β-catenin did not. Surprisingly, the nuclear PKM2 was closely related to CSC-like phenotypes. Taken together, the findings suggest that the PKM2 translocated into the nucleus possibly contributes to CSC-like phenotypes under CUG2 overexpression.

RESULTS

CUG2 increases PKM2 protein levels and induces its translocation to the nucleus

With recent studies documenting that an increase in PKM2 protein levels was observed in clinical tissues, such as lung cancer (19), pancreatic ductal adenocarcinoma (20), colorectal cancer (21), and ovarian cancer tissues (22), we considered the possibility that PKM2 contributes to CSC-like phenotypes induced by CUG2. Here, when the levels of PKM2 protein were compared between the A549-CUG2 and BEAS-CUG2 cells, which are stably expressing CUG2, and A549-Vec and BEAS-Vec cells, PKM2 protein levels were significantly higher in

CUG2 overexpression cells than in the control cells that were stably expressing an empty vector (Fig. 1A). Interestingly, when the endogenous PKM2 was examined, the majority of PKM2 proteins were found in the cytosol, while certain portions of the PKM2 were found in the nuclei of the cells overexpressing CUG2 (Fig. 1B). Furthermore, when the PKM2 was forcibly expressed by the WT PKM-GFP or GFP vector, GFP was found in the nuclei of the cells transfected with WT PKM-GFP vector but GFP was not detected in the nuclei of the cells transfected with GFP vector (Fig. 1C).

Furthermore, when we examined the transcription factors that could be collaborators for nuclear PKM2 (15), (16), we discovered that CUG2 increases levels of c-Myc and CyclinD1 (Fig. 1D). The enforced expression of PKM2 also increased the levels of these proto-oncogenic proteins (Fig. 1D). These results propose that CUG2 induces the upregulation of PKM2, thus leading to transferring of the protein into the nucleus and subsequently collaborating with proto-oncogenic proteins such as c-Myc and CyclinD1.

Both EGFR-ERK and Yap1-NEK 2 signaling transduction increase PKM2 expression

As previously reported, both the EGFR–ERK and the β-catenin-NEK2 signaling transduction via Yap1 are closely related to CSC-like phenotypes mediated by CUG2 (4), (5). As a result, we considered the possibility that these signaling pathways contribute to the increase in PKM2 expression. Once EGFR and ERK inhibitors were administrated under CUG2 overexpression, the reduced levels of PKM2 protein were notified (Fig. 2A). The lower phosphorylation levels of the target proteins also confirmed that these inhibitors were working (Fig. 2A). Furthermore, lower PKM2 protein levels were detected in both cytosol and nucleus after treatment with EGFR and ERK inhibitors compared with treatment with DMSO, confirming that the EGFR-ERK signaling axis is involved in the expression of PKM2 (Fig. 2A). After β-catenin, Yap1,

and NEK2 were suppressed with the attendant siRNA, the PKM2 protein levels were examined. We found that PKM2 protein levels were reduced during Yap1 and NEK2 suppression but that β-catenin suppression did not reduce PKM2 protein expression (Fig. 2B). Therefore, we propose that elevated PKM2 protein levels can be caused by not only increased kinase activity of EGFR and ERK1/2 but also enhanced expression of Yap1 and NEK2.

CSC-like phenotypes are attributed to PKM2 protein under CUG2 overexpression

We wondered whether PKM2 plays an important role in CSC-like phenotypes under CUG2 overexpression such as rapid cell migration, assertive invasion, enhanced ability of sphere formation, and increased resistance to anti-cancer drug, because we discovered the increase of PKM2 protein levels under CUG2 overexpression in previous tests (Fig. 1A). To answer this question, when the PKM2 protein levels were suppressed with the attendant siRNA, the CUG2-induced CSC-like phenotypes were explored. In this case, the PKM2 suppression resulted in the slower migration (Fig. 3A) and invasion (Fig. 3B) compared to control siRNA treatment. Furthermore, PKM2 knockdown reduced both the number and size of spheroids (Fig. 3C). In addition, our previous studies documented that under CUG2 overexpression, resistance to doxorubicin-induced cytotoxicity is closely related to the decrease of reactive oxygen species production (23). Herein, we observed that the cells drastically enhanced ROS production and cleaved PARP levels during PKM2 knockdown, indicating increased sensitivity of apoptosis to doxorubicin (Fig. 3D). Thus, we imply that CSC-like phenotypes are attributed to PKM2 protein under CUG2 overexpression.

Nuclear PKM2 during the enforced expression contributes to CSC-like phenotypes

Because there are numerous lines of evidence that PKM2 protein performs non-metabolic functions in tumor formation (11), (15), (16), (17), (18), we concentrated on

PKM2's role as a co-activator. As a result, we introduced the mutant Ser37A PKM2-GFP that cannot be translocated to the nucleus during EGF stimulation (14). We also observed that the forced expression of the mutant Ser37A PKM2-GFP failed to show PKM2 localization in the cell nuclei (Fig. 4A). To verify that ERK can phosphorylate PKM2 at Ser37 as described previously (14), ERK inhibitor was treated into A549-CUG2 and BEAS-CUG2 cells and phosphorylation levels of PKM2 at Ser37 was examined using a specific phospho-Ser37-PKM2 antibody. We found that treatment with the ERK inhibitor reduced phosphorylation levels of PKM2 at Ser37 (Fig. 4A).

In comparison to WT PKM2-GFP transfection, the mutant Ser37A PKM2-GFP transfection resulted in slower migration and invasion of control cells (Figs. 4B and 4C). Furthermore, the mutant expression of PKM2 exhibited a lower number of smaller-sized spheroids in the cells, compared to WT PKM2-GFP (Fig. 4D). Moreover, the enforced expression of the mutant Ser37A PKM2-GFP induced lower NEK2 kinase activity and β-catenin transcriptional activity compared with the WT PKM2-GFP transfection (Supplementary Fig. 1). Furthermore, WT PKM2-GFP transfection resulted in higher levels of c-Myc and CyclinD1 protein than the mutant PKM2 transfection (Fig. 4E). These findings suggest that PKM2 may have a CSC-like capacity as a co-activator when combined with the proto-oncogenic proteins; c-Myc and CyclinD1.

DISCUSSION

The Warburg effect, a common marker of tumor cell metabolism, is characterized by cancers' increased utilization of glucose and increased production of lactate via the glycolysis pathway even under normal conditions(20% oxygen concentration) (7), (8). With the

documents, the Warburg effect is attributed to behaviors of PKM2 protein (9). Based on these lines of evidence (7), (8), (9) , we performed nuclear magnetic resonance spectroscopy about the CUG2-overexpressing cells and the control cells to determine a difference in glycolytic metabolites and amino acids. Lactate production was not different between A549-CUG2 and A549-Vec cells, but BEAS-Vec produced more lactate than BEAS-CUG2 cells (Supplementary Fig. 2). Because no significant differences in other metabolites were found, we hypothesize that PKM2 does not function as a metabolic enzyme in the aerobic glycolytic pathway.

Because we had observed that PKM2 protein was translocated to the nucleus, we considered the idea that PKM2 protein acts as a co-activator. Previous research has shown that the translocated PKM2 proteins that bind to Jumonji-C-domain-containing dioxygenase Jumonji-containing protein 5 in the nucleus promote HIF-1α expression (16). In addition, other studies have shown that the interaction between PKM2 and c-Src is required for the recruitment to the CyclinD1 promoter during EGFR signaling (17). Moreover, an additional study has reported that nuclear PKM2 protein exerts as a co-activator together with β-catenin to express c-Myc (18). Thus, these lines of evidence support the translocation of PKM2 to the nucleus in the presence of CUG2 overexpression as well as the increased expression of CyclinD1 and c-Myc in the presence of PKM2, as confirmed by PKM2 siRNA treatment and transfection with mutant Ser37A PKM2-GFP (unable to translocate into the nucleus). Since PKM2 phosphorylated histone H3 acts as a protein kinase, which contributes to the development of tumors (13), our findings suggest that PKM2 can carry the ability inducing CSC-like phenotypes such as a speedy cell migration, assertive invasion, and the increased spheroid size and number, which do not rule out a protein kinase role.

Therefore, PKM2 protein has been considered a potential target for cancer therapy.

Treatment with Shikonin, a natural compound derived from *Lithospermum erthrorhizon*, could suppress glycolytic rate that is determined by lactate production and glucose consumption (24), and inhibited 12-O-tetradecanoylphorbol 13-acetate (TPA)-induced cellular transformation and activation of PKM2 (25). Administration of Selumetinib, a MEK inhibitor, diminished phosphorylation of ERK, and prevented EGF-induced nuclear translocation of PKM2, which ultimately suppressed tumor cell growth (14). On the other hand, FFJ-5 and FFJ-3, structurally modified mollugin, attenuated PKM2 expression through EGFR-Akt-PKM2 and PI3K-Akt signaling pathways, respectively (26) (27). These lines of literature support our findings on the oncogenic role of PKM2 under CUG2 overexpression.

MATERIALS AND METHODS

Antibodies and Reagents

Cell Signaling Biotechnology (Danvers, MA, USA) provided antibodies that target β-catenin, EGFR, and ERK1/2, as well as phospho-β-catenin, phospho-EGFR, phospho-ERK1/2, and PKM2. Antibody recognizing phospho-PKM2(Ser37) was purchased at Thermo Fisher Scientific (Walltham, MA, USA). Anti- Yap1 and -NEK2 antibodies were acquired from Abcam (Cambridge, MA, USA). Furthermore, Santa Cruz Biotechnology (Santa Cruz, CA, USA) provided antibodies against CyclinD1 and c-Myc obtained. Finally, gefitinib and PD98059 purchased from Calbiochem (San Diego, CA, USA) was used to inhibit EGFR and ERK1/2 kinase activity, respectively.

Cell culture and Transfection

A549 and BEAS-2B cells purchased from ATCC (Manassas, VA, USA) were stably introduced with wild type (22) CUG2 vector, while the control cells were treated with an

empty vector with the same construct. A549-CUG2 and -Vec cells were maintained in RPMI-1640 whereas BEAS-CUG2 and -Vec cells were kept in DMEM medium. The media additionally contained 10% FBS, 1% penicillin, 1% streptomycin, and G418 (500 µg/ml; Sigma Aldrich, St. Louis, MO, USA) at 37°C and 5% CO_2. After reaching a confluence of 50%-60%, the cells were transfected with siRNAs (Bioneer, Daejeon, Korea) targeting PKM2, β-catenin, Yap1, and NEK2 using Lipofectamine® 2000 (Thermo Fisher Scientific, Carlsbad, CA, USA). The same protocol was applied for the transfection of the cells with wild type (22) PKM2- GFP (Addgene, Watertown, MA, USA) or mutant Ser37A PKM2-GFP vector generated by Bioneer.

Cellular Fractionation

Cellular fractionation was performed as previously mentioned (2). The supernatants were obtained as the soluble fractions, after the cells were treated with a TTN buffer including 0.05% Triton X-100 and centrifuged. Then, the pellets were treated with a RIPA buffer including 0.1% SDS, 1% NP-40, and 0.5% deoxycholic acid, and followed by centrifugation. The nuclear extracts were thereafter obtained.

Wound healing assay

The cells were cultured until they were approximately 80% confluent. The gap was measured by observing the cells under a microscope for 24 h.

Transwell invasion assay

Transwell invasion assay was carried out as formerly mentioned (2),(3). Briefly the cells in the upper well invaded the lower wells containing serum through the coated membrane (BD biosciences). After fixing and staining with hematoxylin–eosin, the images were obtained

then under a microscopy (100× magnification). The experiment was tested in triplicates. The data designate the mean ± the standard deviations (SD)

Sphere forming assay

For six days, the cells treated with expression vectors or siRNAs were incubated in a medium containing 0.4% BSA, EGF (20 ng/mL), basic-FGF (10 ng/mL), and insulin (5 µg/mL). The spheroids in wells with ultra-low attachment were measured and counted under an optical microscope. The assay was tested in triplicates. The data designate the mean ± the SD.

Western blotting

Western blotting was performed as previously explained (2), (3). Proteins were segregated from cell lysates using a 10% SDS-polyacrylamide gel and the gel was then conveyed into nitrocellulose membranes. The membrane was then incubated primary antibodies (1:500-1,000 dilution) and subsequently a horseradish peroxidase-conjugated secondary antibody. The images were obtained after treatment with a peroxidase substrate (Thermo Fisher Scientific).

Immunofluorescence Microscopy

PKM2 protein expression and localization were investigated using immunofluorescence as previously described (2). Anti-PKM2 antibody was added to the cells fixed and permeabilized. Thereafter, the treated cells were incubated with Alexa Fluor 488-conjugated secondary antibody for 1 h. After 4′,6-diamidino-2-phenylindole (DAPI) was added to the cells for staining the nuclei, the images were subsequently visualized with a fluorescence microscope.

Measurement of reactive oxygen species

The intracellular reactive oxygen species levels were measured using a fluorescence

microscope after treatment with 20 μM, 2′,7′-dichlorodihydrofluorescein diacetate (DCF; Molecular Probes, Eugene, OR, USA) for 30 min.

Statistical Analysis

All data are presented in terms of mean ± SD. For comparison between two groups, the results were analyzed using Student's unpaired *t*-test. When the *P*-value is greater than 0.05, the data is considered significant.

ACKNOWLEDGMENTS

This study was supported by the National Research Foundation of Korea (NRF) grant funded by the Korean government (MSIT) (2020R 1F1A 1048183) and the Technology Innovation Program (N0002310 and P0008763) funded by the Ministry of Trade, 511 Industry, and Energy (MOTIE, Korea). This work was also supported by Korea Institute for Advancement of Technology(KIAT) grant funded by the Korea Government(MOTIE) (P0008763, The Competency Development Program for Industry Specialist)

CONFLICTS OF INTEREST

The authors declare that they have no known competing financial interests.

SUPPLEMENTARY DATA

Supplementary data to this article can be found online.

FIGURE LEGENDS

Figure 1. Increase in PKM2 protein levels and PKM2 translocation to the nucleus in CUG2-overexpressing cells

(A, D) Protein levels of PKM2, c-Myc, and CyclinD1 in the cytosol and nuclei or whole cell lysates from A549-CUG2 and BEAS-CUG2 cell, and the control cells were detected by Western blotting after 10% SDS-polyacrylamide gel running. PKM2 expression under CUG2 overexpression was scanned and compared to that in the control cells using Multi-Gauge Ver. 2.1 program. (B) For the endogenous expression and localization of PKM2, the cells were incubated with anti-PKM2 antibody and followed by an Alexa Fluor488-conjugated secondary antibody. DNA was stained with DAPI (C) WT GFP tagged-PKM2 expression was detected 48 h after transfection using a fluorescence microscopy. As a control, GFP was then observed.

Figure 2. The elevated PKM expression is attributed to the upregulation of EGFR–ERK and Yap1-NEK2 signaling

(A, B) The kinase activity of EGFR and ERK1/2, and protein expression of Yap1 and NEK2 were measured by Western blotting after gefitinib (20 μM) or PD98059 (30 μM) treatment, and administration with Yap1 or NEK2 siRNA (200 ng).

Figure 3. Treatment with PKM2 siRNA diminishes CUG2-mediated CSC-like phenotypes

(A) The migrated cells filled in the gaps scratched with a 200 μl tip after transfection with PKM2 siRNA. Cell migration was compared with the cell treated with control siRNA. (B)As the cells treated with PKM2 siRNA invaded from upper to lower wells, the number of the cells on the lower wells was counted after hematoxylin-eosin staining. (**P< 0.01; PKM2 siRNA *vs* the control siRNA). (C) PKM2 siRNA or the control siRNA was added to the cells. The size and number of sphere was measured over six days. A sphere with a diameter greater than 50

μm was a criterion for sphere formation. (**P<0.01; PKM2 siRNA *vs* the control siRNA). (D) After transfection with PKM2 siRNA or the control siRNA, the cells were treated with doxorubicin for 12 h. ROS were detected in the cells using 20 μM of DCF under a fluorescence microscope. Apoptosis was measured by immunoblotting using anti-cleaved PARP antibodies.

Figure 4. Translocalization of PKM2 to the nucleus contributes to the generation of CSC-like phenotypes

(A) Immunofluorescence was used to examine the localization of PKM2 in the transfected cells 36 h post-transfection of the cells with WT PKM2-GFP (2 μg) or mutant Ser37A PKM2-GFP (2 μg). DNA was stained with DAPI. After treatment with ERK inhibitor, the phosphorylation level of PKM2 at Ser37 was detected with the corresponding antibody. (B) After transfection of the cells with WT PKM2-GFP (2 μg) or mutant Ser37A PKM2-GFP (2 μg), the gap closure areas were measured for cell migration under phase-contrast microscopy (100× magnification). (C) The cells treated with WT PKM2-GFP or mutant Ser37A PKM2-GFP invaded from upper to lower wells and the number of cells in the lower wells was counted afer haematoxylin-eosin staining. (**P< 0.01; WT PKM2-GFP *vs* mutant Ser37A PKM2-GFP). (D) After transfection of the cells with WT PKM2-GFP or mutant Ser37A PKM2-GFP, the size and number of spheroid was measured and counted over six days. A spheroid exceeding 50 μm was a criterion for sphere formation. (*P<0.01; WT PKM2-GFP *vs* mutant Ser37A PKM2-GFP; **P<0.01; WT PKM2-GFP *vs* mutant Ser37A PKM2-GFP). (E) Western blotting was used to examine the protein expression of CyclinD1 and c-Myc after transfection with WT PKM2-GFP or mutant Ser37A PKM2-GFP.

REFERENCES

1. Lee S, Gang J, Jeon SB et al (2007) Molecular cloning and functional analysis of a novel oncogene, cancer-upregulated gene 2 (CUG2). Biochemical and biophysical research communications 360, 633-639
2. Kaowinn S, Kim J, Lee J et al (2017) Cancer upregulated gene 2 induces epithelial-mesenchymal transition of human lung cancer cells via TGF-β signaling. Oncotarget 8, 5092
3. Kaowinn S, Seo EJ, Heo W et al (2019) Cancer upregulated gene 2 (CUG2), a novel oncogene, promotes stemness-like properties via the NPM1-TGF-β signaling axis. Biochemical and biophysical research communications 514, 1278-1284
4. Kaowinn S, Kaewpiboon C, Koh SS, Krämer OH and Chung YH (2018) STAT1-HDAC4 signaling induces epithelial-mesenchymal transition and sphere formation of cancer cells overexpressing the oncogene, CUG2. Oncology reports 40, 2619-2627
5. Kaowinn S, Yawut N, Koh SS and Chung Y-H (2019) Cancer upregulated gene (CUG) 2 elevates YAP1 expression, leading to enhancement of epithelial-mesenchymal transition in human lung cancer cells. Biochemical and biophysical research communications 511, 122-128
6. Yawut N, Kaewpiboon C, Budluang P et al (2020) Overexpression of Cancer Upregulated Gene 2 (CUG2) Decreases Spry2 Through c-Cbl, Leading to Activation of EGFR and β-Catenin Signaling. Cancer Management and Research 12, 10243
7. Hsu PP and Sabatini DM (2008) Cancer cell metabolism: Warburg and beyond. Cell 134, 703-707
8. Dong G, Mao Q, Xia W et al (2016) PKM2 and cancer: The function of PKM2 beyond glycolysis. Oncology letters 11, 1980-1986
9. Dayton TL, Jacks T and Vander Heiden MG (2016) PKM 2, cancer metabolism, and the road ahead. EMBO reports 17, 1721-1730
10. Whitfield JR and Soucek L (2012) Tumor microenvironment: becoming sick of Myc. Cellular and Molecular Life Sciences 69, 931-934
11. Gao X, Wang H, Yang JJ, Liu X and Liu Z-R (2012) Pyruvate kinase M2 regulates gene transcription by acting as a protein kinase. Molecular cell 45, 598-609
12. Yang P, Li Z, Fu R, Wu H and Li Z (2014) Pyruvate kinase M2 facilitates colon cancer cell migration via the modulation of STAT3 signalling. Cellular signalling 26, 1853-1862
13. Gernapudi R, Yao Y, Zhang Y et al (2015) Targeting exosomes from preadipocytes inhibits preadipocyte to cancer stem cell signaling in early-stage breast cancer. Breast cancer research and treatment 150, 685-695
14. Yang W, Zheng Y, Xia Y et al (2012) ERK1/2-dependent phosphorylation and nuclear translocation of PKM2 promotes the Warburg effect. Nature cell biology 14, 1295-1304
15. Luo W, Hu H, Chang R et al (2011) Pyruvate kinase M2 is a PHD3-stimulated coactivator for hypoxia-inducible factor 1. Cell 145, 732-744
16. Wang H-J, Hsieh Y-J, Cheng W-C et al (2014) JMJD5 regulates PKM2 nuclear translocation and reprograms HIF-1α–mediated glucose metabolism. Proceedings of the National Academy of Sciences 111, 279-284
17. Yang W, Xia Y, Ji H et al (2011) Nuclear PKM2 regulates β-catenin transactivation upon EGFR activation. Nature 480, 118-122

18. Wu H, Li Z, Yang P, Zhang L, Fan Y and Li Z (2014) PKM2 depletion induces the compensation of glutaminolysis through β-catenin/c-Myc pathway in tumor cells. Cellular signalling 26, 2397-2405
19. Wang C, Zhang S, Liu J et al (2020) Secreted pyruvate kinase M2 promotes lung cancer metastasis through activating the integrin Beta1/FAK signaling pathway. Cell reports 30, 1780-1797. e1786
20. Xu Q, Wu N, Li X et al (2019) Inhibition of PTP1B blocks pancreatic cancer progression by targeting the PKM2/AMPK/mTOC1 pathway. Cell death & disease 10, 1-15
21. Bian Z, Zhang J, Li M et al (2018) LncRNA–FEZF1-AS1 promotes tumor proliferation and metastasis in colorectal Cancer by regulating PKM2 signaling. Clinical Cancer Research 24, 4808-4819
22. Ahmed A, Dew T, Lawton F et al (2007) M2-PK as a novel marker in ovarian cancer. A prospective cohort study. European journal of gynaecological oncology 28, 83-88
23. Kaowinn S, Jun SW, Kim CS et al (2017) Increased EGFR expression induced by a novel oncogene, CUG2, confers resistance to doxorubicin through Stat1-HDAC4 signaling. Cellular Oncology 40, 549-561
24. Chen J, Xie J, Jiang Z, Wang B, Wang Y and Hu X (2011) Shikonin and its analogs inhibit cancer cell glycolysis by targeting tumor pyruvate kinase-M2. Oncogene 30, 4297-4306
25. Yue G, Sun X, Gimenez-Capitan A et al (2014) TAZ is highly expressed in gastric signet ring cell carcinoma. BioMed research international 2014
26. Wei X, Li M, Ma M et al (2017) Induction of apoptosis by FFJ-5, a novel naphthoquinone compound, occurs via downregulation of PKM2 in A549 and HepG2 cells. Oncology letters 13, 791-799
27. Li D, Wei X, Ma M et al (2017) FFJ-3 inhibits PKM2 protein expression via the PI3K/Akt signaling pathway and activates the mitochondrial apoptosis signaling pathway in human cancer cells. Oncology letters 13, 2607-2614

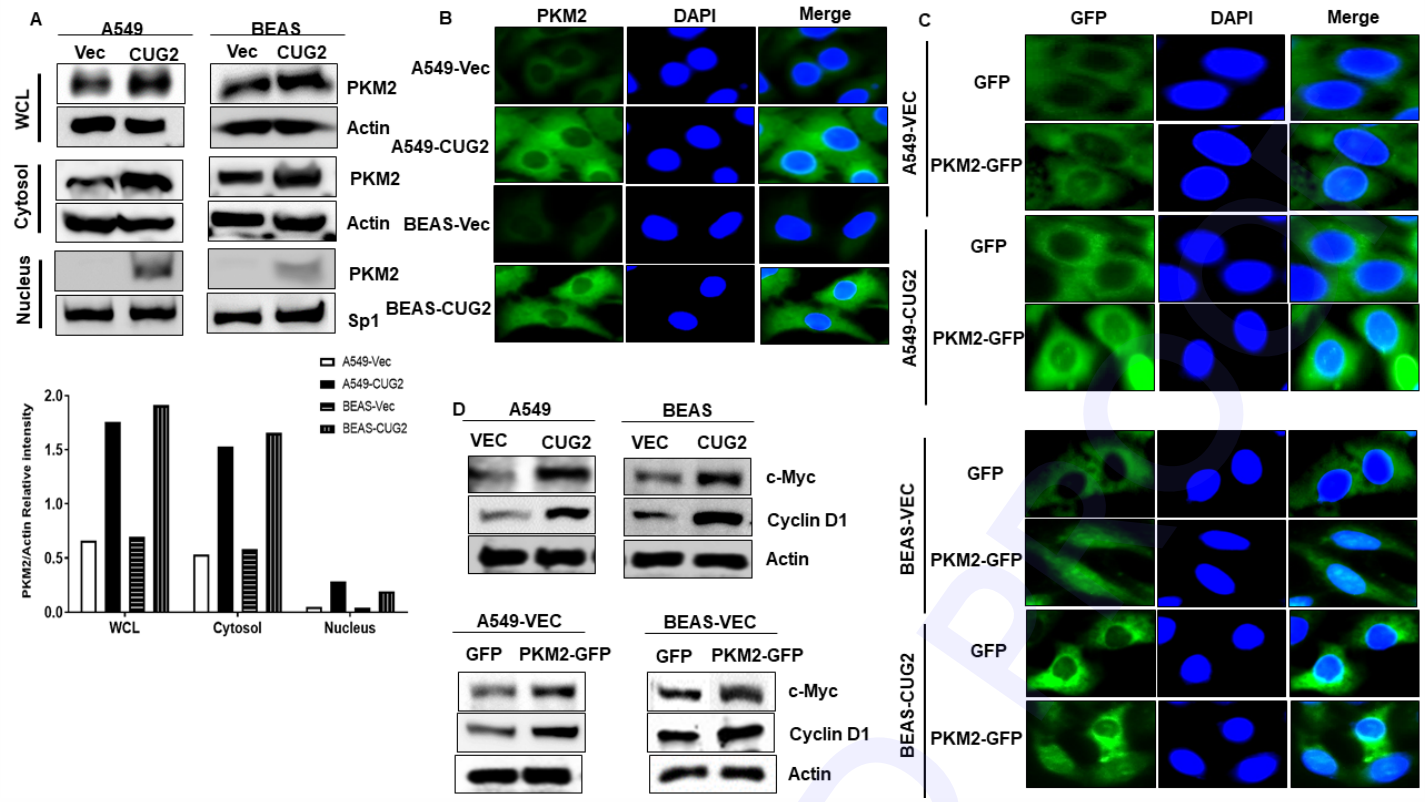

Fig. 1. Figure 1

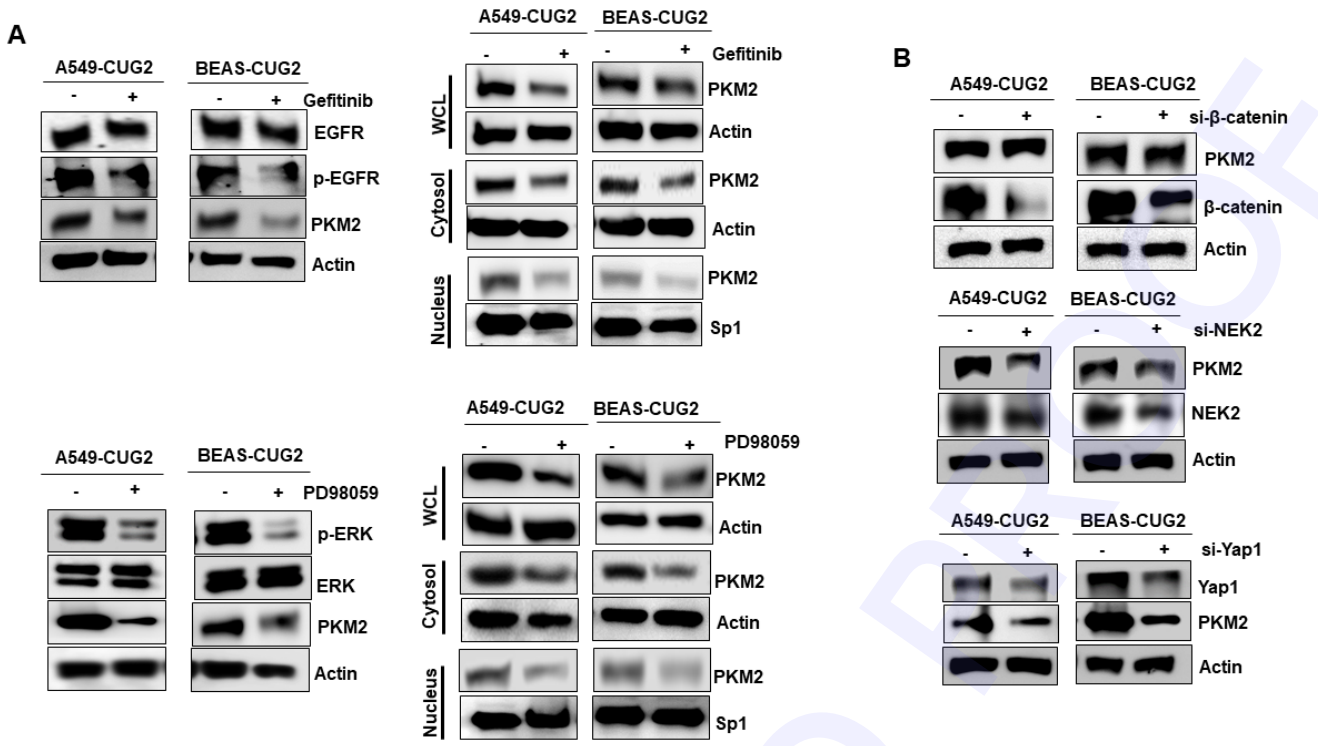

Fig. 2. Figure 2

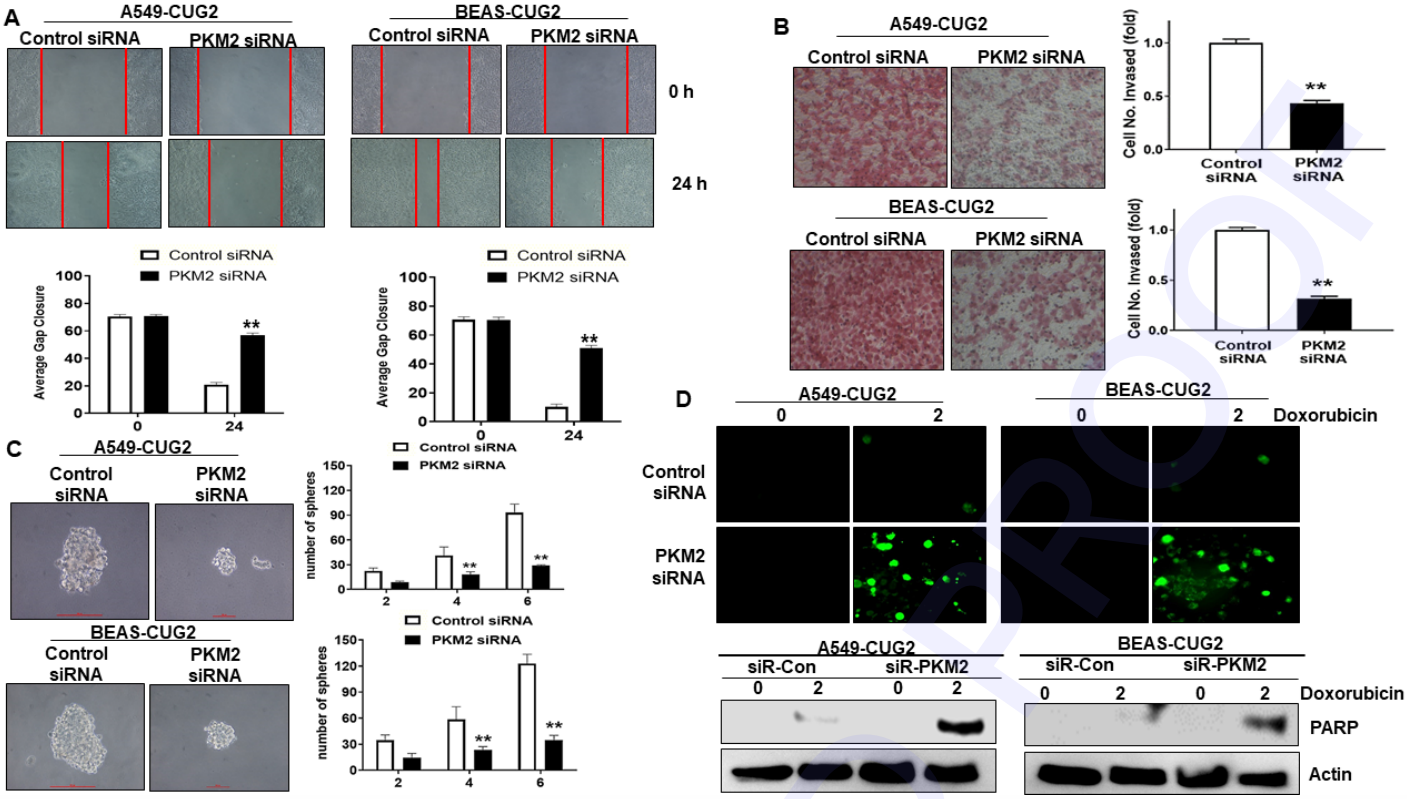

Fig. 3. Figure 3

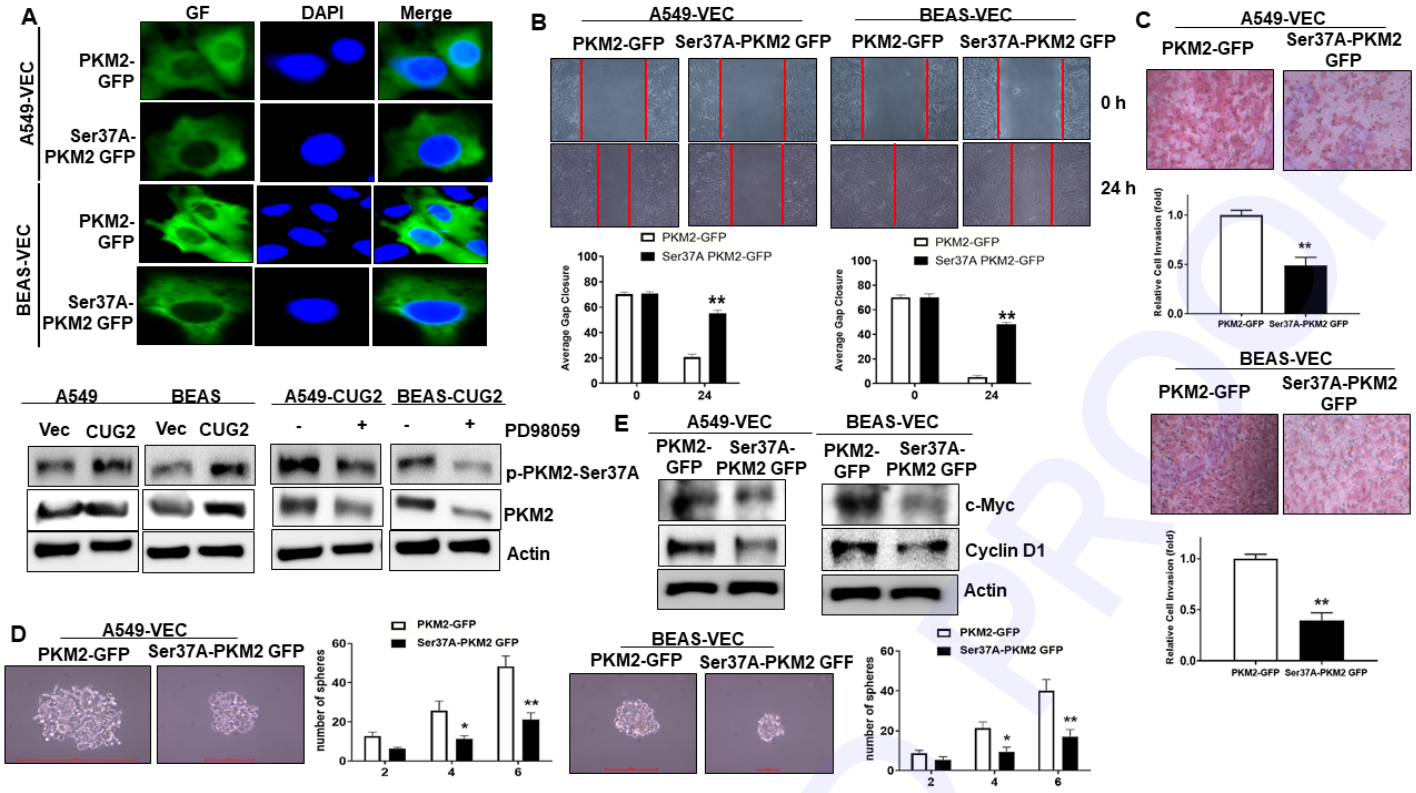

Fig. 4. Figure 4

Translocalization of enhanced PKM2 protein into the nucleus induced by cancer upregulated gene 2 confers cancer stem cell-like phenotypes

Natpaphan Yawut[1a], Sirichat Kaowinn[2a], Il-Rae Cho[1], Phatcharaphon Budluang[1], Seonghye Kim[3], Suhkmann Kim[3], So Eun Youn[4], Sang Seok Koh[4], and Young-Hwa Chung[1*]

[1]BK21 plus, Department of Cogno-Mechatronics Engineering, Optomechatronics Research Center, [3]Department of Chemistry, Pusan National University, Busan 46241, Republic of Korea

[2]Department of General Science and Liberal Arts, King Mongkut's Institute of Technology, Ladkrabang Prince of Chumphon Campus, Chumphon 86160, Thailand

[4]Department of Biomedical Sciences, Dong-A University, Busan 49315, Republic of Korea

Keywords: CUG2, PKM2, cancer stem cell, non-metabolic function

a ; These authors contributed equally to this work

* Corresponding author; Young-Hwa Chung, PhD, Department of Cogno-Mechatronics Engineering, Optomechatronics Research Center, Pusan National University, Busan 46241, Republic of Korea, *Email* ; younghc@pusan.ac.kr

Supplementary Figure 1

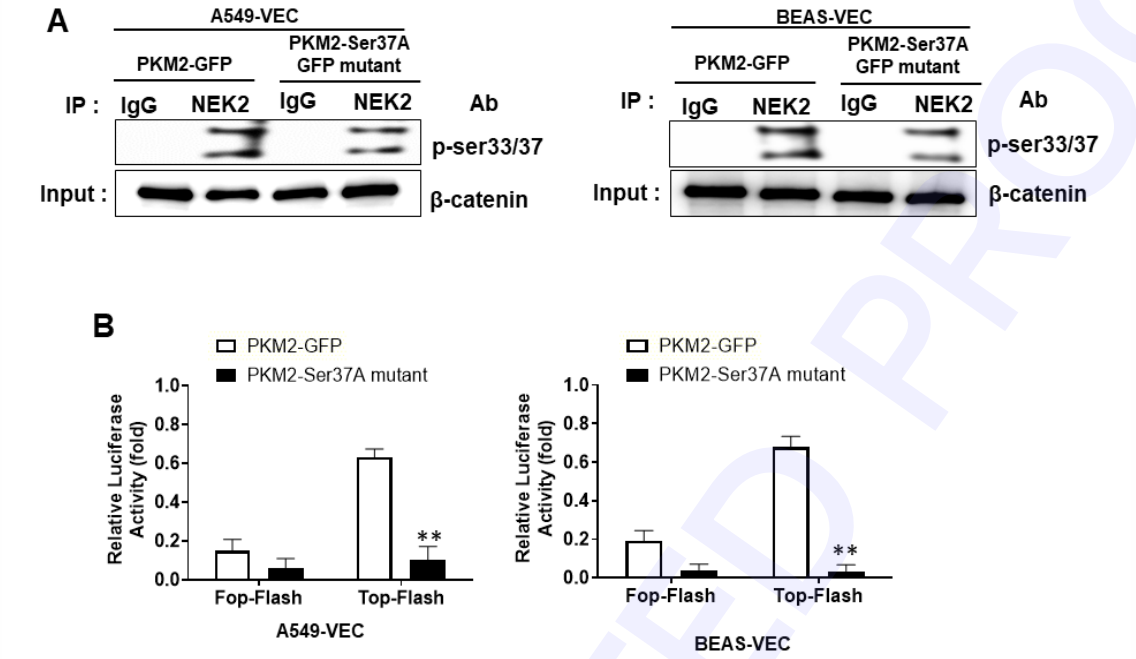

Enforced expression of WT PKM2 enhances NEK2 and β-catenin transcription activities

(A) After immunoprecipitation from the cells transfected with WT PKM2-GFP or mutant Ser37A PKM2-GFP vector using anti-NEK2 antibody, GST-β-catenin (1 μg) and 10 mM ATP (2 μl) were introduced. NEK kinase activity from the reaction mixture was determined by the phosphorylation levels of the position of Ser33/Ser37 of GST-β-catenin after 10% SDS polyacrylamide gel running (B) After transfection of the cells with WT PKM2-GFP or mutant Ser37A PKM2-GFP vector, activity of luciferase was analyzed with a luciferin substrate. (**P<0.01, WT PKM2-GFP *vs* mutant Ser37A PKM2-GFP).

Supplementary Figure 2

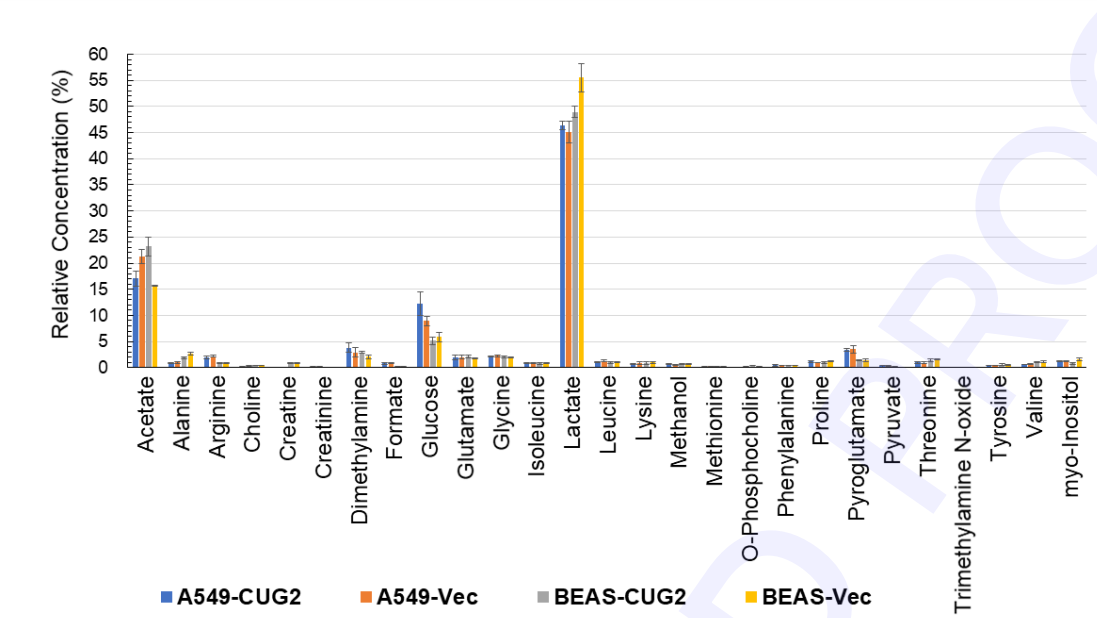

Metabolite identification using NMR measurements

Samples were measured using a 600 MHz HR-MAS NMR spectrometer with a nano-NMR probe (Agilent Technologies, Santa Clara, CA, USA). The 20 mg of sample were weighed and placed into a 4 mm HR-MAS NMR nanotube with 20 µl of phosphate buffer (pH 7.4) in deuterated water (D_2O) containing 2mM 3-(trimethylsilyl) propionic-2,2,3,3-d4 acid sodium salt (TSP-d_4). TSP-d_4 (0 ppm) was used as internal chemical shift standard. The spinning rate was set as 2050 Hz and the CPMG (Carr–Purcell–Meiboom–Gill) pulse sequence was applied to suppress the signal of water and macromolecules. Spectra were acquired using 8.05 µs 90◦ pulse, 1.5 s relaxation delay, 3 s acquisition time, and 13 min total acquisition time with 128 total transients for each sample. The spectra were manually phased and baseline corrected using VnmrJ 4.2 software (Aligent Technologies, Santa Clara, CA, USA). Relative concentrations of metabolites were calculated by normalizing to the sum of total concentrations to reduce sample-to-sample variation.